Journal of Engineering Science and Technology
Vol. 17, No. 1 (2022) 0452 - 0471

HIGH PERFORMANCE OF POWER TRANSFER IN HYBRID AC-DC MICROGRID WITHOUT STORAGE SYSTEM

HASTI AFIANTI[1,2,*], ONTOSENO PENANGSANG[1], ADI SOEPRIJANTO[1]

[1]Department of Electrical Engineering, Institut Teknologi Sepuluh Nopember, Arief Rahman Hakim Road, Keputih CAus, Sukolilo 60111, Surabaya, Indonesia
[2]Electrical Engineering Study Program, Universitas Bhayangkara Surabaya Ahmad Yani Road, Surabaya 60231, Indonesia
*Corresponding Author: zenno_379@yahoo.com, adisup@ee.its.ac.id

Abstract

This paper aims to look at the use of an intermittent renewable energy source (RES) connected to the grid in a hybrid alternating current (AC) - direct current (DC) microgrid concept, without a storage system. It is known that intermittent RES sometimes has excess energy and sometimes lacks, so this condition requires a storage system. A way to solve this problem is to use an AC-DC bidirectional converter as an interlinking converter (IC). The IC connected DC and AC sub microgrids. It also manages the power transfer in the system. The control uses three inputs, the Vage from the DC sub microgrid, the Vage and current from the AC sub microgrid. The control uses pulse width modulation (PWM) and also d-q rotating coordinate system. What is new from this research is that the Vage from the AC sub microgrid is only used for input to the phase lock loop (PLL). This is to maintain the converter phase shift equal to the network. The simulation was built on Simulink / Matlab and adding power changes in the DC sub microgrid and the load changes in the AC sub microgrid. The results prove that the built-in IC works on the systems with stable Vages, frequencies, and the total harmonic distortion (THD) is less than 8% that meets the Institute of Electrical and Electronics Engineers (IEEE) Standard 519TM-2014 requirements. The efficiency of the IC is reaches 99.4% as a rectifier and 99.6% as an inverter. The contribution of the proposed study can provide better performance than the previous study by showing the power transfer between ac and dc sub microgrid with eliminating delay and overshoot.

Keywords: Bidirectional converter, Hybrid AC-DC microgrid, Grid connected, Power transfer, Without storage system.

1. Introduction

Until now, the fulfilment of electrical energy depends on long-distance transmission systems from sources with giant power plants, and electricity generated using AC power, but when electricity will enter electronic equipment, AC power is converted to DC power by the adapter, like laptops, handphones, etc. This conversion is inefficient because there is wasted energy. To be efficient, of course, the electrical system must come from a DC source as well, like on DC House [1]. In DC House, the conversion of AC to DC is not needed because electricity from DC House can be directly used. Another major advantage of DC House is flexibility. In its basic design, DC House is designed to be able to receive electricity from any source, such as wind, water, solar and even people who ride bicycles. So, an area can utilize the most abundant potential electricity source. This desire is very difficult to implement, considering the electricity system that is currently developing is the AC system.

A new electricity concept, distribution generators that supply the surrounding load into a subsystem or microgrid of the distribution system makes the starting point of change in the conventional electricity [2]. Research on microgrid has been growing in almost two decades. AC microgrid, DC microgrid, and a combination of them was known as hybrid AC-DC microgrids. On AC microgrid there are main buses that use the AC system as well as on DC microgrids where the main bus uses the DC system. In both types of microgrid, both source and load will use the system on the main bus type. Different from AC and DC microgrid, in hybrid AC-DC microgrid, AC load will be connected and supplied with an AC source, and also the DC load which will be connected and supplied with a DC source, because it is directly connected to the same source, this system can reduce the use of converter [3]. This reduction is in line with the reduction of harmonic pollution and increasing the power quality of the system, also increase the installed power [4-6].

In this system there are two central buses, DC bus, and AC bus, and they connected with interlinking converter as illustrated in Fig. 1. The interlinking converter has a very important role. This power electronics equipment is expected to be able to flow power from AC microgrid to DC microgrid if the power generated by a DC source cannot supply the load power requirements, conversely, if a DC source produces excess power from the DC load requirements, the interlinking converter must be able to transfer this excess power to the AC microgrid to be traded. For this reason, the interlinking converter should use bidirectional converter, this converter must have the ability to be a rectifier or an inverter, conduct power in both directions properly because in addition to power change there is also load change on the system.

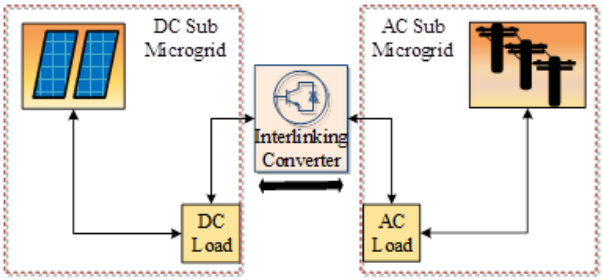

Fig. 1. Hybrid AC-DC microgrid.

The converter expected to be able to flow power better from. DC to AC or AC to DC sub microgrid according to the power changes of the sub microgrid. Some previous studies have given results but need to be improved. The bidirectional converter with only Vage control from AC sub microgrid not yet able to regulate the power flow with changes in power and load conditions, but it can drain the power when a three-phase disturbance occurs [7]. By using the SVPWM, d-q rotating coordinate system and setting the value of quadrature current equal to zero is not yet able to perform a two-way power transfer [8].

Table 1. The comparison between previous and proposed study.

No.	Authors	Methods	Change mode	Delay	Over shoot
1	Eghtedarpour and Farjah [6]	PWM, d-q rotating coordinate system, two-stage modified droop control	√	√	√
2	Afianti et al. [7]	PWM, d-q rotating coordinate system, input from AC terminal Vage	×	×	×
3	Huang et al. [8]	SVPWM, d-q rotating coordinate system, and setting i_q	×	×	×
4	Mohammed et al. [9]	SPWM, d-q rotating coordinate system, the Vage from the AC side used for input in the PLL and current control	√	√	×
5	Liu et al. [10]	PWM, d-q rotating coordinate system, coordination between boost and main converter	√	√	√
6	Alias et al. [11]	Change the IGBT topology and switching technique	√	×	×
7	Loh et al. [12]	PWM, d-q rotating coordinate system, droop control in DC and AC sub sides	√	√	×
8	Zheng et al. [13]	SPWM, d-q rotating coordinate system, droop control in the DC side	√	√	×
9	Proposed Study	PWM, d-q rotating coordinate system, the AC terminal Vage is only used for input in the PLL	√	×	×

Note : × = not available, √ = available

A vector decoupling-controlled SPWM rectifier has been designed and implemented to connect the DC system to the grid. The study was conducted using a Vage from the AC sub microgrid as input for the PLL and current control. The power transfer can run well even though there is still a delay [9]. The proposed study is very near to this method, the difference is that the Vage of the AC sub microgrid is only used for input on the PLL, which is simpler than [9]. The coordination control strategies between boost and main converter are verified the

hybrid grid can operate stably in the grid-tied or isolated mode under various generation and load conditions [10]. The bidirectional converter with modified 6-switch topology and PWM switching technique can regulate the bidirectional power flow [11]. The results obtained from this method are as good as the proposed method, it can already show a change in mode from rectifier to the inverter or vice versa by eliminating delay and overshoot. A unified control strategy using droop control schemes has been proposed for ensuring proportional power-sharing throughout an autonomous hybrid microgrid [12-13].

These researches use three inputs from the AC and DC sub microgrid, Vage from DC sub microgrid, Vage and current from AC sub microgrid and other modification [6, 9, 10, 12-14]. The same thing was done in this study. The controls able to change the mode of the converter when the current was changed from positive to negative that indicate the current flow is changed, the simulation results show that there is a phase shift of current to the Vage of 180^0 even there are delay and overshoot in the simulation as mentions in Table 1. This table shows a comparison of the methods and results for several previous studies and the proposed study. The observed results include a change in mode from rectifier mode to the inverter mode or vice versa and the occurrence of delay or overshoot when the mode change occurs. It is shown that the contribution of the proposed study has better results than several previous studies. The proposed study can regulate the bidirectional power transfer without delay and overshoot with the simplest control.

In this paper, the hybrid AC DC microgrid system was built by Simulink / Matlab with the bidirectional converter as an interlinking converter. The built system is connected to a grid without a storage system. The IC control uses three inputs, the Vage from the DC sub microgrid, the Vage and current from the AC sub microgrid. The methods used PWM and d-q rotating coordinate system. What is new from this research is the Vage of the AC sub microgrid is only used for input on the PLL. This is done to maintain the converter phase shift equal to the network. This study complements previous research by connecting the system to the grid and adding variations in power and load changes. The simulation is carried out by providing power and load changes to prove the control performance of the bidirectional converter working without delay and overshoot when mode switching occurs in the converter. This paper consists of several sections, in Section 2 described the system configuration with the bidirectional converter followed by simulation and discussion in Section 3 and the conclusion in Section 4.

2. Hybrid AC-DC microgrid with Bidirectional Converter as Interlinking Converter

2.1. Hybrid AC-DC microgrid system

In this system consists of 3 large circuits: DC sub microgrid, AC sub microgrid and interlinking converter. The DC sub microgrid consists of DC source inheriting the photoVaic (PV) and fuel cell connected with a load, some exAle for DC load are light emitting diode (LED), and modern elevator. In AC sub microgrid side has a grid-connected with many kinds of load combination. Because each sub microgrid has a load that must be supply, a good converter is needed that can maintain power stability in the event of a power shortage, especially in the DC sub microgrid, given the intermittent nature of the RES and in this research the system does not use an energy storage system. The use of energy storage system becomes a dilemma when

a RES is connected to a stable grid. As has been widely applied that the use of RES is rarely separated from the energy storage system, where it is used to reserve power requirements because of the intermittent of the RES. However, the energy storage system, like a battery, is not very economical, because the battery has a short lifetime (between 3 and 5 years maximum in rural areas for solar lead-acid batteries which are commonly used for RES), and must be recycled, technology to recycle batteries is very rare so that batteries that are not used will become junk if left longer, and batteries has a big shape, this will certainly harm the environment, chemical pollution, and high investment.

Some researchers with their research based on the concept of "flexy energy" proved on techno-economic that a hybrid system between PV and diesel generators without using a storage system has higher effectiveness than stand-alone of diesel generators system [15-18]. As well as has been researched that PV applied on the roof-top or building integrated photoVaic (BIPV) and grid without storage is techno-economic has high effectiveness because the cost of energy (COE) decreases in line with the increase in power capacity [19]. From all this research, it can be concluded techno-economic that hybrid PV systems can work on the grid or off-grid even without a storage system, but this system requires a converter that not only can flow current properly but also can work as rectifier and inverter so it can maintain Vage and frequency stability, despite changes in power and load.

While in the hybrid AC DC microgrid connected to the main utility grid as an AC source. The grid expected to be able to supply active and reactive power to the network both on the AC sub microgrid side and DC sub microgrid system. In this case, beside the grid will maintain the power balance, both active, and reactive power, the grid will maintain the stability of the Vage and frequency in the system. Figure 2 shows a series of systems built in this study. In the DC sub microgrid, there is a DC source with a load and a capacitor link. In the AC sub microgrid, there is also an AC source in this case in the form of a grid, load, and LCL filter. The notation and parameters used in the system are listed in Appendix *A*. To connect the two sub microgrids, there is an interlinking converter with the controls described in Section 2.2.

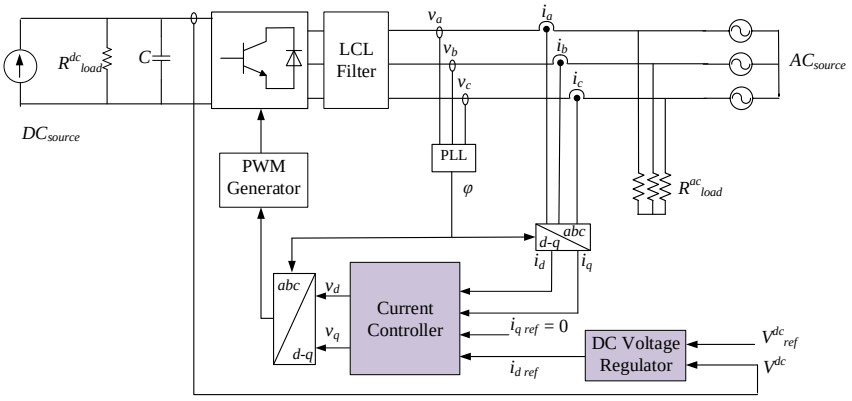

Fig. 2. The overall configuration of the proposed system.

In the hybrid AC DC microgrid, the AC and DC sub microgrid have separate power equations [20]. Regardless of the power loss, the power on the DC sub

microgrid with N_A is the number of DC buses. $P_{load}^{dc,h}$ is power demand of h^{th} load in DC sub microgrid. $P_{source}^{dc,h}$ is power generated by h^{th} energy source in DC sub microgrid. P_{loss}^{dc} is power loss in DC sub microgrid and P_{IC}^{dc} is power transfer from AC to DC or DC to AC that through the IC. The power in the DC sub microgrid can be expressed as follows [20, 21]:

$$0 = \sum_{h=1}^{N_A} P_{load}^{dc,h} + P_{loss}^{dc} + P_{ic}^{dc} - \sum_{h=1}^{N_A} P_{source}^{dc,h} \quad (1)$$

where the generator, load, reactive power compensator, AC lines and the converter are connected on the bus *i* as depicted in Fig 3.

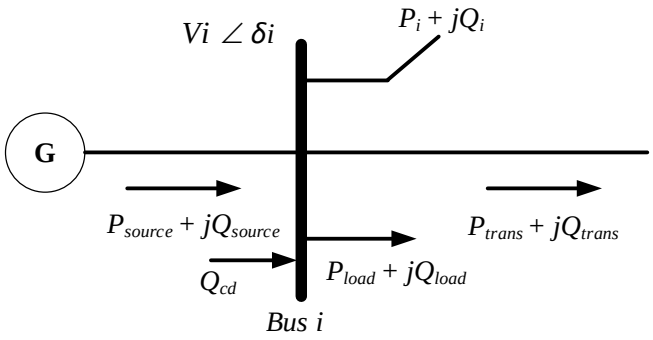

Fig. 3. General AC bus presentation.

The active and reactive power balance equations at AC sub microgrid can be expressed as follows [22]:

$$P_{source}^{ac} - P_{load}^{ac} - s_p P_{ic}^{ac} - V_i \sum_{j=1}^{N_B} V_j \left(G_{ij} cos\delta_{ij} + \quad B_{ij} sin\delta_{ij}\right) = 0 \quad (2)$$

$$Q_{source}^{ac} + Q_{cd} - Q_{load}^{ac} - s_q Q_{ic}^{ac} - V_i \sum_{j=1}^{N_B} V_j \left(G_{ij} sin\delta_{ij} + B_{ij} cos\delta_{ij}\right) = 0 \quad (3)$$

where $P_{source}^{ac} + Q_{source}^{ac}$ and $P_{load}^{ac} + Q_{load}^{ac}$ are complex power of the generator and load respectively. Q_{cd} is the output of the reactive power compensation device, V_i and δ_i are the Vage magnitude and angle. $G_{ij} + B_{ij}$ where is the i jth element of the admittance matrix of the AC power network, N_B is the number of AC buses. $s_p = 0$ and $s_q = 0$ if no converter is connected at bus , $s_p = 1$ and $s_q = 1$ if the converter at bus is a rectifier, $s_p = -1$ and $s_q = -1$ if the converter at bus is an inverter [23].

The Vage line to line ($V_{ab}^{ac}, V_{bc}^{ac}, V_{ca}^{ac}$) in the three-phase converter with naturally sAled PWM, with the three sinusoidal references displaced in time by 120^o [24].

$$V_{ab}^{ac} = M\sqrt{3}V^{dc} \cos(\omega_o t + \frac{\pi}{6}) \quad (4)$$

$$V_{bc}^{ac} = M\sqrt{3}V^{dc} \cos(\omega_o t - \frac{\pi}{2}) \quad (5)$$

$$V_{ca}^{ac} = M\sqrt{3}V^{dc} \cos(\omega_o t + \frac{5\pi}{6}) \quad (6)$$

where M is the modulation index (the normalized output Vage magnitude) of the IC with the range $0 < M < 1$ and ω_o is target output angular frequency [23].

The relation between the DC power and the AC active power is a function of the efficiency of the converter, ignoring switching losses in the converter, as follows [19].

$$P^{ac} = \frac{P^{dc}}{\mu^{IC}} \tag{7}$$

In Eq. (7), P^{ac} and P^{dc} is the power in the AC and DC interface of the IC and μ^{IC} is the efficiency of the IC.

2.2. Proposed interlinking converter control

This interlinking converter connects DC sub microgrid and AC sub microgrid. The converter uses 6 insulated gate bipolar transistor (IGBT), the input control comes from both sides, on the side of the AC sub microgrid using current and Vage, and the Vage on the DC sub microgrid side. With inputs that are on the two sides of the converter, the converter can work bidirectionally as a rectifier or inverter, converting DC power into AC power and vice versa, depending on the power situation of both sub microgrids.

Described in Fig. 4, the Vage from the AC sub microgrid becomes reference input is of the PLL to synchronize the phase angle. The PLL circuit in this system is modelled as a closed-loop system that monitors the variation of the phase angle using an internal oscillator. The control system adjusts the internal oscillator to keep the phases difference to zero. Using Park Transform, the phase angle generated by the internal oscillator is used to change the three phase Vage from AC sub microgrid into dq coordinates.

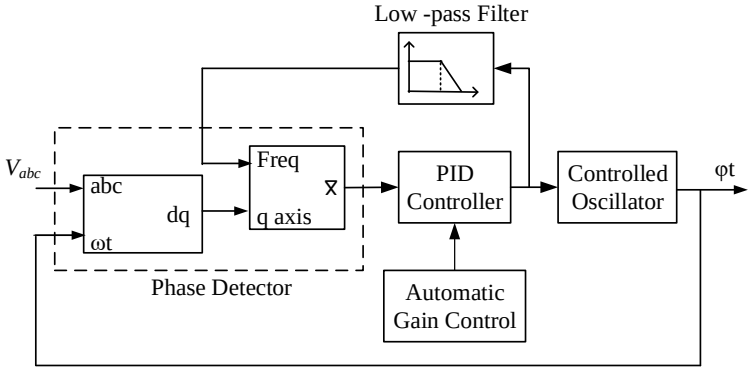

Fig. 4. Phase lock loop.

The Mean (Variable Frequency) block computes the mean value of the quadrature signal, $f(t)$. This average value is obtained from one frequency cycle of the quadrature signal, with T = 1/frequency.

$$Mean\left(f(t)\right) = \frac{1}{T}\int_{(t-T)}^{t} f(t).dt \tag{8}$$

The output of the mean block combine with optional automatic gain control (AGC) becomes the input of the proportional integral derivative (PID) controller. This controller keeps the phase difference to 0. The PID output, according to the angular velocity, is filtered and converted to a frequency that is used to find the average value. While the phase angle generated by PLL is used to transform the

abc to dq coordinates or dq to abc coordinates as seen in Fig. 2, the AC sub microgrid current is change to dq coordinate and becomes input of the current control of as seen in Fig. 5.

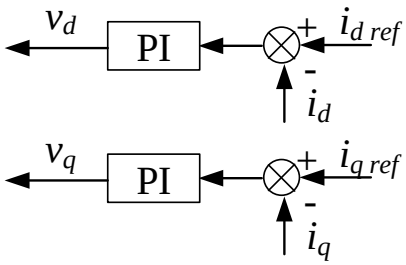

Fig. 5. Current controller.

The close loop DC Vage is control with the set point of DC reference Vage, which is then controlled by the PI controller and determine with $i_{d\,reff}$ as described in Fig. 6. Besides the PI controller, the value of $i_{d\,reff}$ depends on the limiter. The constant limiter value specified as the maximum and minimum values as in Eq. (9).

$$i_{d\,reff} = \begin{cases} i_{d\,reff} & ; -C_{min} < i_{d\,reff} < C_{max} \\ -C_{min} & ; \quad i_{d\,reff} < -C_{min} \\ C_{max} & ; \quad i_{d\,reff} > C_{max} \end{cases} \tag{9}$$

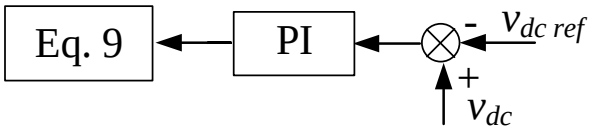

Fig. 6. DC Vage regulator.

The sum of i_d and i_q from the current loop with $i_{d\,reff}$ and $i_{q\,reff}$ are controlled by the PI controller and change to abc coordinate with Park Transformation, before becoming an input of the PWM modulator. Finally, the PWM modulator produces pulses that move the switch on IGBTs in the interlinking converter.

3. Results and Discussion

3.1. The simulation

The system modeling is done as shown in Fig. 2. During the simulation, there are power changes in DC sub microgrid and load changes on the AC sub microgrid. The simulation is carried out for 6 seconds with a schedule of power changes as shown in Figs. 7 and 8 there is a schedule of load changes. The change in power gradually follows the gauss curve pattern like the average shape of solar radiation every day.

The analysis of the simulation was carried out in 2 places in the DC microgrid and AC microgrid. The flowchart of the simulation shown in Fig. 9, from the flowchart It appears that the mode change on the IC is very dependent on the source and load conditions on the DC sub microgrid.

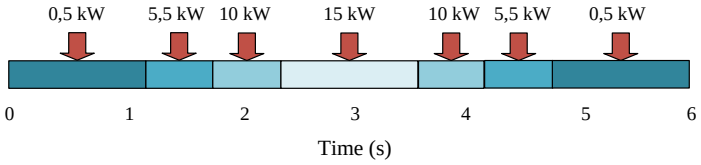

Fig. 7. The schedule of power changes.

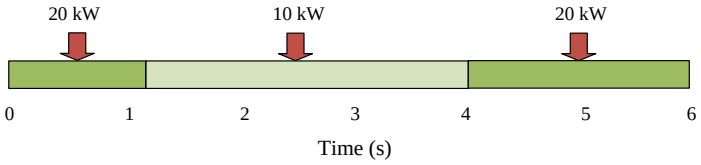

Fig. 8. The schedule of load changes.

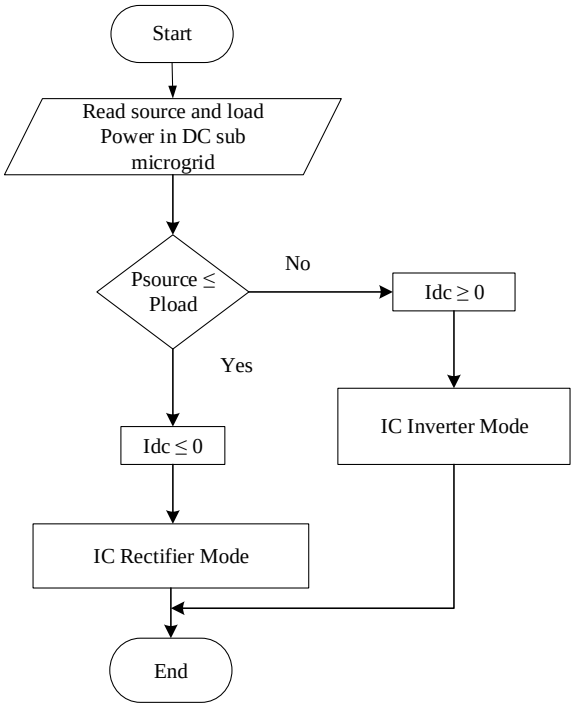

Fig. 9. Flowchart of the simulation.

3.2. DC sub microgrid

With power change at the DC source, there is also a change in current and Vage at the DC sub microgrid, as seen in Fig. 10 for the current and Fig. 11 for the Vage response. When there is a decrease in DC source power that cannot supply dc power load in 0 s until 1.8 s, makes the current becomes negative, this indicates that the dc power load supplied from the IC, it is mean that the IC become rectifier. When the DC power source starts to increase in 1.8 s until 2.4 s, even where the DC source is greater than the DC load, the current becomes positive.

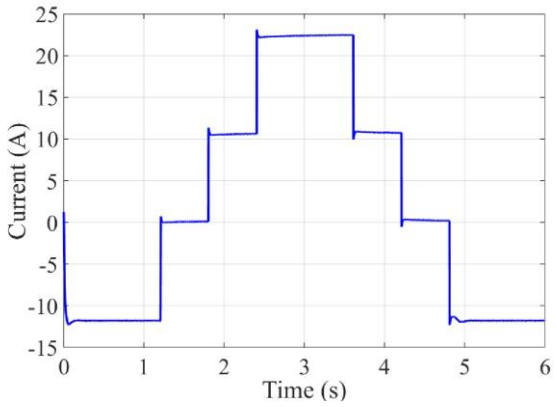

Fig. 10. DC sub microgrid current.

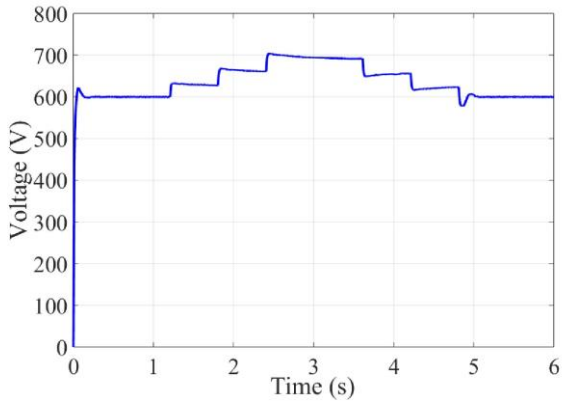

Fig. 11. DC sub microgrid Vage.

In this case, the IC will get power supply from the DC source and make the IC function as an inverter. When the power source decrease but it still bigger than dc load power in 3.6 s until 4.2 s, the current is still positive, and the IC still becomes an inverter. It is different when the source power still decreases until less than load power in 4.2 s until 6 s, the current becomes negative, and the IC function becomes a rectifier again. Changes in DC power source cause changes in DC Vage, this is normal, because the model of this simulation using a controlled current source module to reflect on resources. Controlled current source module was supplied by P_{dc} as DER that setting like in Fig. 6 and divided with V_{reff}^{dc} that in this simulation was setting in 400 V.

Figure 12 shows the power flow at the DC Source, DC load, and the power transferred through the IC. In this figure, the power comparison was described very clear, when DC power is very small and even close to zero then the IC will transfer power to supply the load power requirements, so the value of the power transfer becomes negative. If the load power is equal to the DC power, the IC does not transfer power, this can be seen from the value of the power transferred by the IC close to zero. Conversely, when the DC power is greater than the load power the power transferred from the IC becomes positive, this indicates that the DC microgrid is delivering power to the IC.

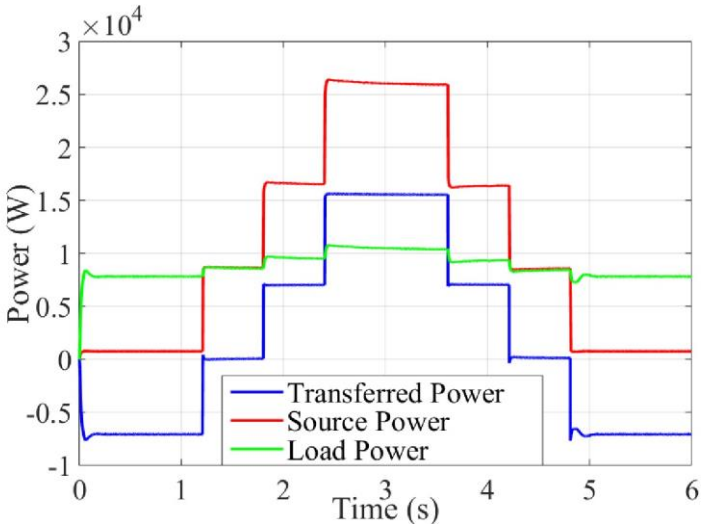

Fig. 12. DC sub microgrid power with DC Vage regulator.

3.3. AC sub microgrid

The impact of power changes on the DC source can be seen not only in the DC sub microgrid but also in the AC sub microgrid. Fig. 13(a) shows the Vage and current that occurs in the AC sub microgrid during the simulation. With power change on the DC sub microgrid and the load on the AC sub microgrid according to Figs. 7 and 8 make the IC function changed as a rectifier or inverter following the changes that occur in the system. In the Fig. 13(a) to Fig. 13(g) the Vage on the AC sub microgrid is maintained properly despite changes in power and load.

Different things happen to the current, the AC sub microgrid current changed not only in its magnitude but also a phase angle shift. Fig 13(b) until Fig. 13(f) is an enlargement of the Fig. 13(a), which is cut every second to show the current changes. Enlargement from 0 s to 1 s is described in Fig. 13(b), in this figure the Vage and current are stable because there is still no power or load change. The Vage and current are in a different phase, it indicates that the IC in rectifier mode. Power from DC source is insufficient to supply the DC load power requirements and thus requires power supply from the AC sub microgrid. In Fig. 13(c) especially at 1.2 s to 1.8 s the DC power start increases almost match to the load requirements, the current near to zero, indicating that there is less power flow from the IC to the load, and there has been a phase shift between current and Vage around 90^{o}.

At 1.8 s, there was a power increase in the DC sub microgrid which exceeds the DC load requirements. This excess power flowing through the IC to AC sub microgrid and the function of the IC changes to an inverter, in this case, the current and Vage in one phase. In Fig. 13(d) there was a DC power increase again at 2.4 s this changes the amount of current but does not change the IC function. In the 3.6 s, there was a reduction in DC power, the current also decreases but does not change the IC function because there is still power transfer from IC to AC sub microgrid. The current is still one phase with the Vage, this is shown in Fig. 13(e). In Fig. 13(f) show a reduction in DC power source at 4.2 s to 4.8 s that the DC power only supplies DC load requirements.

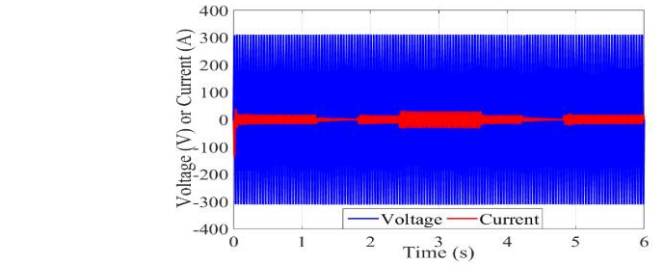

(a) Result of the whole simulation

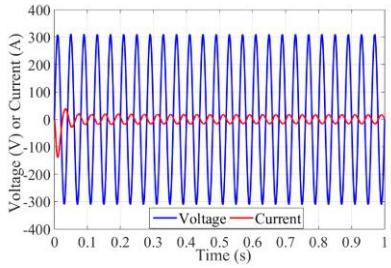

(b) The result from 0 s to 1 s

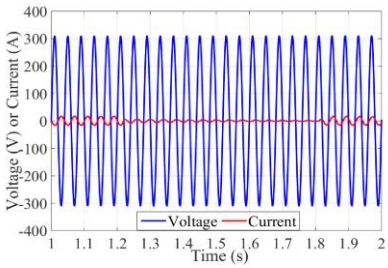

(c) The result from 1 s to 2 s

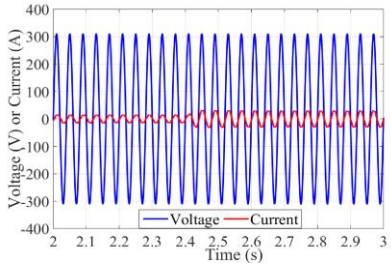

(d) The result from 2 s to 3 s

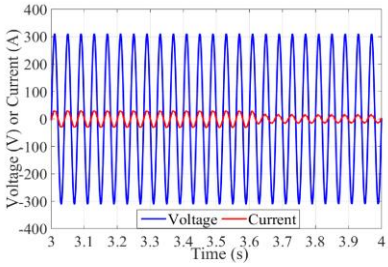

(e) The result from 3 s to 4 s

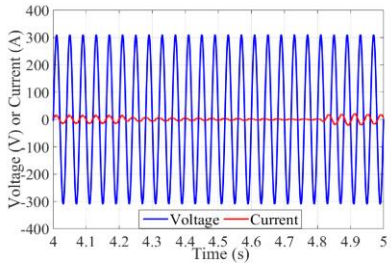

(f) The result from 4 s to 5 s

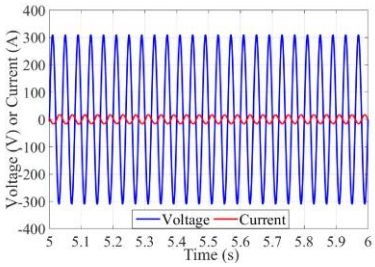

(g) The result from 5 s to 6 s

Fig. 13. Vage and current in AC sub microgrid.

This power reduction causes the IC cannot supply power to the AC sub microgrid. At this time the current almost zero, and there is a phase shift with a Vage of around 90º. Then the DC power decreases again at 4.8 s shown in Fig. 13(g) until the DC source is unable to supply the load power requirements. This power reduction causes a phase shift between current and Vage of 180º, the IC changes to a rectifier. Besides the Vage and current that can show the change of IC function, the active power flow also can do that. In Fig. 14 illustrates the comparison of active power at load, source, and power transferred to DC sub microgrid. The DC power changes make the power transferred in the AC sub

microgrid become negative that is mean the IC transferred the power into the DC sub microgrid, the IC becomes rectifier, and vice versa when the transferred power becomes positive that is mean the IC transfer power into AC sub microgrid, the IC becomes inverter.

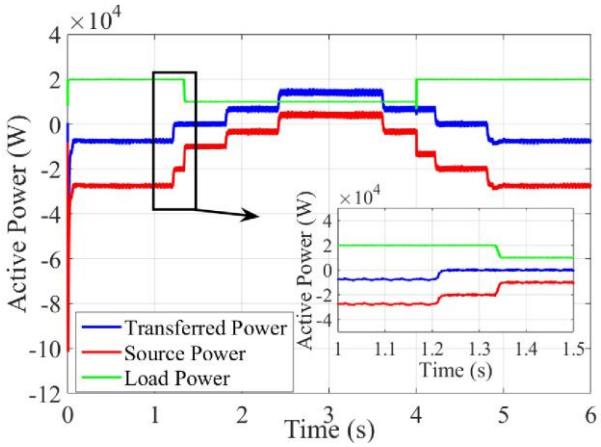

Fig. 14. Comparative of active power in AC sub microgrid.

The AC source power is negative, means the grid supplies power to the system, and when the DC power increase, the grid gets power supply from the system, it changes the AC power source to positive. The Load changes during simulation that occur on the AC sub microgrid as a scenario in Fig. 8 do not have much impact on the power transferred to the DC sub microgrid. But with the change in load on the AC sub microgrid, it can be seen that even though the power transferred is not sufficient for the load requirements, the power requirements at the load will be met by the source power from the AC sub microgrid, in this case, the grid.

Figure 15 shows the reactive power during the simulation. Reactive power at the source and interface converter on the AC side follows the power changes that happen at the DC sub microgrid. They have the same value until difficult to recognize. When there is a decrease in the load power on the AC sub microgrid, it will have an overshoot effect even though it is small on the reactive power from the source.

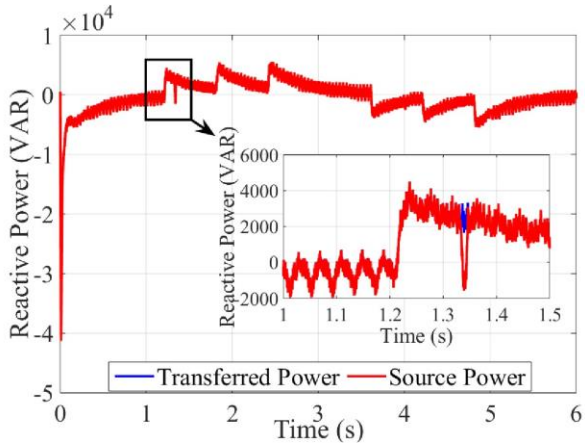

Fig. 15. The transferred and source reactive power in AC sub microgrid.

Figure 16 shows the reactive power that occur in the load. In this simulation, there are three load combinations, the first is starting from 0 s to 1.2 s, there is a combination between resistive and inductor, the second is starting from 1.2 s to 4 s, that there is only resistive, and the third is starting from 4 s to 6 s, there is a combination between resistive and capacitor. The value of the reactive power in this system was very small when compared to the active power.

Figure 17 shows the comparison of the power transferred by DC sub microgrid and AC sub microgrid. It can be seen from the picture that the power transferred between the two sub microgrids is almost the same and can even be said to be the same because the power difference is very small. Changes that occur in the system during the simulation affect to the system harmonics, although not significant, this can be seen from Fig. 18. It is seen that the THD value shows the changes following the power changes that occur in the DC sub microgrid. The THD value during the simulation takes no more than 8%, as in t = 3 s, at that time the THD system was only 0.4%. This is in accordance with the provisions of the IEEE Std 519TM-2014 standardization, where at a Vage of less than or equal to 1KV, the THD cannot be more than 8%. Likewise, what happened at the system frequency during simulation, the frequency value was relatively stable, as in the t = 3 s, it can be seen that the frequency is 50 Hz, although there was a ripple when there was a power change in the DC sub microgrid, this can be seen from the simulation results in Fig. 19.

Table 2. Show the efficiency of the converter in a rectifier and inverter. This table proves that the converter can work very efficiently because the efficiency of the converter is very high. However, this converter still has difficulty in maintaining its work efficiency in the same AC and DC sub-microgrid power conditions or in the power transfer condition equal to zero. This can be seen from its rather low efficiency of 80.04% at a sub-microgrid DC power of 5.5 kW compared to its efficiency at 15 kW which is 99.6%. This has never been considered by previous study and should be a concern for further research development.

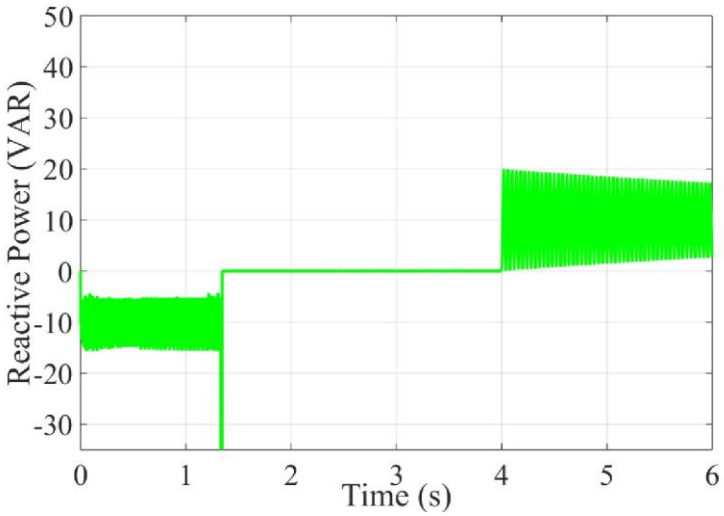

Fig. 16. The load reactive power in AC sub microgrid.

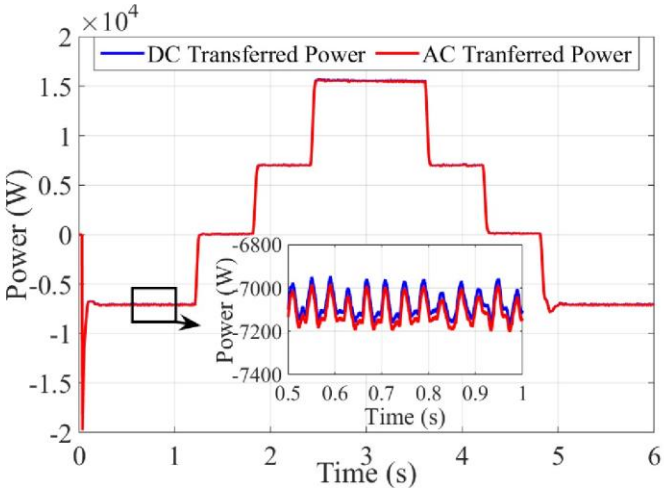

Fig. 17 The comparative of AC and DC transferred power.

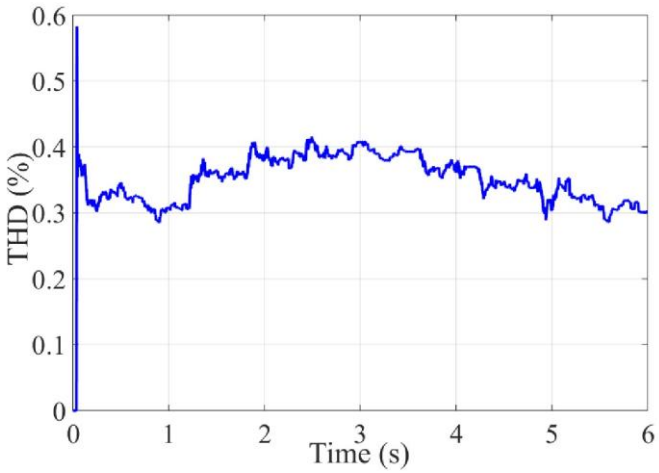

Fig. 18. THD.

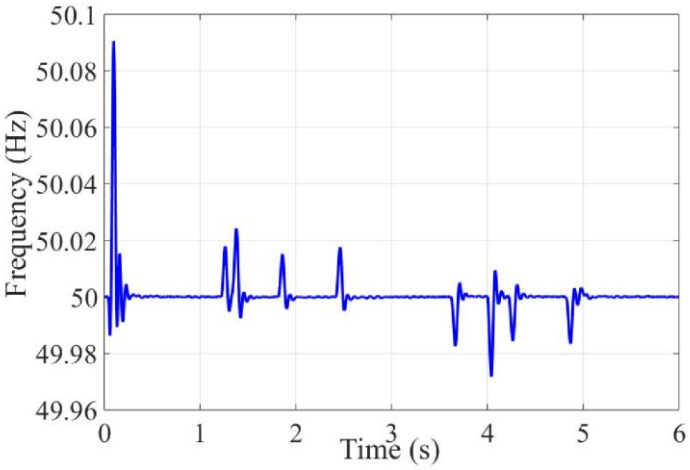

Fig. 19. Frequency of the system.

Table 2. The IC efficiency.

$P^{dc}{}_{source}$	P^{dc}	P^{ac}	μ^{IC}	IC Mode
0.5×10³	-6335	-6374	99.4%	Rectifier
5.5×10³	-67.99	-84.94	80.04 %	Rectifier
10×10³	8682	8642	99.5%	Inverter
15×10³	18980	18910	99.6%	Inverter

The simulation is carried out by changing the power with a graded pattern and the load with a pattern similar to the daily load, but this is still far from being compared to the real conditions in the field. As we know that renewable energy is very intermittent, not only changes over time, even its existence is lost for a while, such as sunlight at night on the use of solar systems or the presence of water in the dry season on microhydro. Apart from the source side of DG there are also constraints from the load conditions. Where the load model should be more varied due to conditions in the field that very varied, both in terms of type and quantity. Not to mention if there is a disturbance in the system, to prove the reliability of the proposed control, further research is needed taking into account. the real conditions in the field, even though it is in the form of a simulation. So that when the implementation is carried out, it is hoped that the proposed control can meet the needs in real conditions.

4. Conclusions

In this paper, the AC-DC hybrid microgrid system has been built using a bidirectional converter that functions as an IC.

- IC is built with a very simple with d - q rotating coordinate system method, but the simulation results show that the system can work very well because ICs with high efficiency can be a rectifier or inverter to respond the power changes that occur in the system without delay and overshoot. The efficiency of the IC reaches 99.4% as rectifier and 99.6% as inverter.
- Load changes that occur in the AC sub microgrid do not affect the power transferred through the IC but occur in the grid or AC source.
- Despite changes in power and load, the Vage and frequency on the system remain stable, THD is no more than 8%.

The power transfer between AC and DC sub microgrid that manage by the IC that based on bidirectional converters make the system run well, power requirement can be met despite the lack of power, especially in the DC sub microgrid. The IC can transfer power, either active or reactive power from the DC sub microgrid to the AC sub microgrid and vice versa. So it can be said that this system has a high performance in power transfer.

Abbreviations

AC	Alternating Current
AGC	Automatic Gain Control
BIPV	Building Integrated PhotoVaic
COE	Cost of Energy
DC	Direct Current
DER	Distributed Energy Resources

IC	Interlinking Converter
IEEE	Institute of Electrical and Electronics Engineers
IGBT	Insulated Gate Bipolar Transistor
LED	Light Emitting Diode
PID	Proportional Integral Derivative
PLL	Phase Lock Loop
PV	PhotoVaic
PWM	Pulse Width Modulation
RES	Renewable Energy Source
SPWM	Sinusoidal Pulse Width Modulation
SVPWM	Space Vector Pulse Width Modulation
THD	Total Harmonic Distortion

References

1. Taufik, M.; and Taufik, T. (2015). UNPAD's DC house prototype to showcase an alternative solution to rural electrification. *Proceeding of International Conference on Rural Development and Community Empowerment*, Bandung, Indonesia.
2. Lasseter, R.H.; and Paigi, P. (2004). Microgrid: A conceptual solution. *Proceedings of* 2004 *IEEE* 35*th Annual Power Electronics Specialists Conference* (*PESC'*04), Aachen, Germany.
3. Afianti, H.; Penangsang, P.; and Soeprijanto, A. (2015). Management strategy of hybrid microgrid to reduce multiple conversion. *Proceeding of International Conference on Electrical Engineering, Informatics and Its Education* 2015 (*CEIE*- 2015), Malang, Indonesia.
4. Park, S.-H.; Choi, J.-Y.; and Won, D.-J. (2014). Cooperative control between the distributed energy resource in AC/DC hybrid microgrid. *Proceedings of Innovative Smart Grid Technologies Conference* (*ISGT*), Washington DC, USA.
5. Long, B.; Jeong, T.W.; Lee, J.D.; Joong, Y.; and Chong, K.T. (2015). Energy management of a hybrid AC-DC micro-grid based on a battery testing system. *Energies*, 8(2), 1181-1194.
6. Eghtedarpour, N.; and Farjah, E. (2014). Power control and management in an AC/DC hybrid microgrid. *IEEE Transactions on Smart Grid*, 5(3), 1494-1505.
7. Afianti, H.; Ashari, M.; Penangsang, P.; Soeprijanto. A.; and Suyanto (2016). Power transfer enhancement in hybrid AC-DC microgrids. *Journal of Engineering and Applied Sciences*, 11(7), 1660-1664.
8. Huang, L; Chen, X.; Xiao, L.; Gong, C. (2009). Research on the bi-directional AC-DC converter for the large non-grid-connected wind power application. *Proceedings of the* 2009 *World Non-Grid-Connected Wind Power Energy Conference*, Nanjing, China.
9. Mohamed, A.; Elshaer, M.; and Mohammed, O. (2011). Bi-directional AC-DC/DC-AC converter for power sharing of hybrid ac/dc system. *Proceedings of Power & Energy Society, IEEE General Meeting*, Detroit, MI, USA.
10. Liu, X; Wang, P; Loh, P.C. (2011). A hybrid AC/DC microgrid and its coordination control. *IEEE Transaction on Smart Grid*, 2(2), 278-286.
11. Alias, A.; Rahim, N.A.; Hussain, M.A. (2011). Bidirectional three phase power converter. Proceedings of the 2011 *IEEE First Conference on Clean Energy and Technology* (*CET*), Kuala Lumpur, Malaysia.

12. Loh, P.C.; Li, D.; Chai, Y.K.; and Blaabjerg, F. (2013). Autonomous control of interlinking converter with energy storage in hybrid AC-DC microgrid. *IEEE Transactions on Industry Applications*, 49(3), 1374-1381.
13. Zheng, X.; Gao, F.; Ali, H.; and Liu, H. (2017). A droop control based three phase bidirectional ac-dc converter for more electric aircraft applications. *Energies*, 10(3), 400.
14. Afianti, H.; Penangsang, P.; and Soeprijanto, A. (2020). Stability and reliability of low Vage hybrid ac-dc microgrids power flow model in islanding operation. *Indonesian Journal of Electrical Engineering and Computer Science*,19(1), 32-41.
15. Azoumah, Y.; Yamegueu, D.; Ginies, P.; Coulibaly, Y.; and Girard, P. (2011). Sustainable electricity generation for rural and peri-urban populations of sub-Saharan Africa: the ''flexy-energy'' concept. *Energy Policy*, 39(1), 131-141.
16. Tsuanyo, D.; Azoumah, Y.; Aussel, D.; and Nevel, P. (2015). Modeling and optimization of batteryless hybrid PV (photoVaic)/Diesel systems for off-grid applications. *Energy*, 86, 152-163.
17. Yamegueu, D.; Azoumah, Y.; Py, X.; and Zongo, N. (2011). Experimental study of electricity generation by solar PV/diesel hybrid systems without battery storage for off-grid areas. *Renewable Energy*, 36(6), 1780-1787.
18. Yamegueu, D; Azoumah, Y.; Py, X.; and Kottin, H. (2013). Experimental analysis of a solar PV/diesel hybrid system without storage: focus on its dynamic behavior. *International Journal of Electrical Power & Energy Systems*, 44(1), 267-274.
19. Tomar, V.; and Tiwari, G.N. (2017). Techno-economic evaluation of grid connected PV system for households with feed in tariff and time of day tariff regulation in New Delhi - A sustainable approach. *Renewable and Sustainable Energy Reviews*, 70, 822-835.
20. Ahmed, H.M.A.; Eltantawi, A.B.; and Salama, M.M.A. (2018). A generalized approach to the load flow analysis of AC-DC hybrid distribution systems. *IEEE Transactions on Power Systems*, 33(2), 2117-2127.
21. Baradar, M.; Hesamzadeh, M.R.; and Ghandari, M. (2013). Second-order cone programming for optimal power flow in VSC-type AC-DC grids. *IEEE Transactions on Power Systems*, 28(4), 4282-4291.
22. Yu, J.; Yan, W.; Li, W.; Chung, C.Y.; and Wong, K.P. (2008). An unfixed piecewise-optimal reactive power-flow model and its algorithm for AC-DC systems. *IEEE Transactions on Power Systems*, 23(1), 170-176.
23. Li, Q.; Liu, M.; and Liu, H. (2015). Piecewise normalized normal constraint method applied to minimization of Vage deviation and active power loss in an ac-dc hybrid power system. *IEEE Transactions on Power Systems*, 30(3), 1243-1251.
24. Holmes, D.G.; and Lipo, T.A. (2003). *Pulse* width modulation for power converters*: Principles and practice*. New York: A John Wiley and Sons Inc.

Appendix A

The Simulation Model and Parameter

A.1. Parameter of the Simulation

This is parameter of the simulation: In the three phase sources: RMS Vage 380 V (line-line), 50 Hz; In the LCL filter and DC link: converter side inductance L_1 = 1 mH converter side resistance, R_1 = 0.5 Ω, grid side inductance L_2 = 1 mH, grid side resistance R_2 = 0.5 Ω, shunt capacitance C_2 = 1 µF, shunt resistance R_2 = 2 Ω, Capacitor filter C = 1500 µF; In DC source and load: DC load resistance R_{dc} = 46 Ω; DC Vage V_{DCreff} = 400 V.

A.2. Model of the Simulation

The simulation using Simulink / Matlab, and the model Simulink described in Fig. A-1.

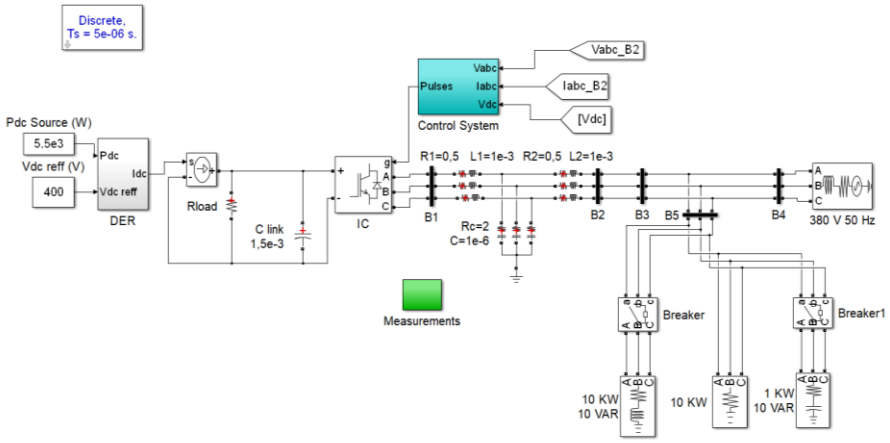

Fig. A-1. Model of the simulation.

Appendix B

The Simulations Measurement Results and Calculations

B.1. DC Sub Microgrid Data

The data in Table B-1 displays the Vage, current and power generated from the measurement of every change in DC sub microgrid. The data is taken at the source, load and interface of the converter on the DC side.

Table B-1. DC sub microgrid data.

DC Source (W)	DC Source			DC Load			DC Transferred		
	V (V)	*I* (A)	*P* (W)	*V* (V)	*I* (A)	*P* (W)	*V* (V)	*I* (A)	*P* (W)
$0.5\ 10^3$	601	1.25	751.3	601	13.07	7852	601	-10.54	-6335
$5\ 10^3$	619.4	12.5	7743	619.4	13.47	8341	619.4	-0.109	-67.99
$10\ 10^3$	659.3	25	16480	659.3	14.33	9451	659.3	13.17	8682
$15\ 10^3$	693.7	37.5	26010	693.7	15.08	10460	693.7	27.36	18980

B.2. AC Sub Microgrid Data

Table B-2 is the result of Vage, current, in the source, load, and interface converter measurements on the AC side. These measurements are made for any changes in DC power. Whereas the active and reactive power values from the data in table B-2 are obtained from calculations using the formula as in Eq. (B-1) for active power and Eq. (B-2) for reactive power.

$$P = V_a I_a + V_b I_b + V_c I_c \quad \text{(B-1)}$$

$$Q = \left(\frac{1}{\sqrt{3}}(V_{bc} I_a + V_{ca} I_b + V_{ab} I_c)\right) \quad \text{(B-2)}$$

where V_a, V_b, V_c are the phase Vage to the ground. I_a, I_b, I_c are the phase current, V_{ab}, V_{bc}, V_{ca} are inter-phase Vages.

Table B-3 is the result of active and reactive power in the source, load, and interface converter on the AC side

Table B-2. AC sub microgrid Vage and current data.

DC Source (kW)		Vage			Current		
		V_a (V)	V_b (V)	V_c (V)	I_a (A)	I_b (A)	I_c (A)
0.5	Source	-1.106	-268.6	269.7	3.304	50.6	-53.9
	Load	269.7	-268.6	-1.106	37.35	-37.17	-0.179
	Transferred	199.7	-401.2	201.5	6.132	10.56	-16.69
5	Source	-0.841	-267.1	268	1.495	36.95	-38.45
	Load	268	-267.1	-0.841	37.11	-36.98	-0.139
	Transferred	205.8	-413.4	207.6	2.896	0.1284	-3.025
10	Source	-2.63	-266.8	269.4	1.07	24.8	-25.87
	Load	269.4	-266.8	-2.63	37.31	-36.93	-0.388
	Transferred	219.1	-438.2	219.1	2.604	-13.15	10.54
15	Source	-1.266	-268.2	269.5	-1.599	11.75	-10.15
	Load	269.5	-268.2	-1.266	37.32	-37.12	-0.201
	Transferred	231.8	-461.7	229.9	1.111	-27.34	26.23

Table B-3. AC sub microgrid power data.

DC Source (kW)		Power	
		P (W)	Q (VAR)
0.5	Source	-28140	-1440
	Load	20050	-12.18
	Transferred	-6374	-7912
5	Source	-20170	-637.7
	Load	19820	-10.53
	Transferred	-84.94	-2120
10	Source	-13590	-381.4
	Load	19910	-11.13
	Transferred	8642	3013
15	Source	-5882	768.4
	Load	20010	-12.1
	Transferred	18910	10090